NMR Studies on the N-Terminal Acetylation Domain of Histone H4

Eunjung Bang,[†‡] Chang-Hun Lee,[§] Jong-Bok Yoon,[§] Joohee Chung,[‡] Dai Woon Lee,[†,*] and Weontae Lee[§,*]

[†]*Department of Chemistry, Yonsei University, Seoul 120-749, Korea*
[‡]*Korea Basic Science Institute, Seoul Branch, Seoul 136-701, Korea*
[§]*Department of Biochemistry and Protein Network Research Center, Yonsei University, Seoul 120-749, Korea*
Received February 8, 2001

Histones, nuclear proteins that interact with DNA to form nucleosomes, are essential for both the regulation of transcription and the packaging of DNA within chromosomes. The N-terminal domain of histone H4 which contains four acetylation sites at lysines, may play a separate role in chromatin structure from the remainder of the H4 chain. NMR data suggest that $H4^{NTP}$ peptide does have relating disordered structure at physiological pH, however, it has a defined structure at lower pH conditions. The solution structure calculated from NMR data shows a well structured region comprising residues of Val21-Asp24. In addition, our results suggest that the $H4^{NTP}$ prefers an extended backbone conformation at acetylation sites, however, it (especially Lys^{12}) became more defined structures after acetylation for its optimum function.

Keywords : Histone H4, Acetylation, NMR structure.

Introduction

Histones (H2A, H2B, H3 and H4) and DNA constitute the nucleosomes, which are essential in packaging eukaryotic DNA into chromosomes. Both stability and positioning of chromatin structures determine repression or activation of nucleosome transcription.[1,2] Restructuring of chromatin often involves alterations in DNA-histone contacts within the nucleosome, or alterations in contacts between nucleosomes that affect higher-order structures. For example, removal of the positive charge of lysines in the N-terminal domains of all four core histones occurs by a dynamic process known as histone acetylation. The rate of acetylation process has also been correlated with gene expression in many systems.[1,3] By contrast, removal of acetyl groups by opposing histone deacetylase (HD) activities restores positive charges of histone protein, which correlates best with transcriptionally silent chromatin.[4,5] The amount of histone acetylation is determined by an equilibrium between histone acetyltransferases (HAT) and histone deacetylases (HDAC). Therefore, it has been reported that chromatin structure could be reversibly modulated to activate or silence transcription by targeting histone acetyltransferases or deacetylases to a particular gene.[6] The recent clonings of the catalytic subunits of a HAT B in the yeast *Saccharomyces cerevisiae*,[7] a HAT A in *Tetrahymena*[8] and a HD from mammals[9] provide both direct and indirect connections between transcriptional activation and histone acetylation. As acetylation neutralizes the positively charged lysine residues of the histone N termini, it decreases their affinity for DNA. In addition, this acetylation might allow termini to be displaced from the nuclesome, causing the nucleosomes to unfold and easy access to transcription factors. In fact, acetylated lysine residues in the N-terminal domains of nucleosomal histones are considered as landmarks for transcriptionally active chromatin within the chromosome.[10] The acetylation, particularly of histone H4, has also been proposed to play an important role in replication-dependent nucleosome assembly. Antibodies against specific acetylation sites in histone H4 have been used to show that potentially active euchromatin can be modified at all the H4 acetylable lysines (Lys5, Lys8, Lys12 and Lys16), whereas H4 in hetero-chromatin is found to be hypoacetylated.[11,12] It was also reported that newly synthesized H4 was preferentially acetylated at Lys5 and Lys12, suggesting that acetylation pattern is closely correlated with its assembly.[13] Figure 1 shows sequence of the histone H4 N-termini. The four acetylation sites in the N-terminal domain of H4 are indicated as circles.

Here, we present the structural characterizations of N-terminal domains of histone H4 ($H4^{NTP}$) using NMR spectroscopy. In addition, we will discuss the conformational change due to acetylation of histone H4.

Experimental Section

Peptides Synthesis. The N-terminal 27 residues of histone H4 (Ser1-Gly2-Arg3-Gly4-Lys5-Gly6-Gly7-Lys8-Gly9-Leu10-Gly11-Lys12-Gly13-Gly14-Ala15-Lys16-Arg17-His18-Arg19-Lys20-Val21-Leu22-Arg23-Asp24-Asn25-Ile26-Gln27) ($H4^{NTP}$) and acetylated histone H4 (Ace-$H4^{NTP}$) were synthesized commercially (KBSI, Seoul branch). The purified peptides were finally characterized by combined use of high performance liquid chromatography (HPLC) and mass spectrometry (MS).

NMR Spectroscopy. Samples used for NMR experiments were 2-20 mM concentration ranges and dissolved in 90% H_2O/10% D_2O solutions. The sample pH was adjusted to

*To whom correspondence should be addressed: Weontae Lee, Ph.D. (Tel: +82-2-2123-2706, Fax: +82-2-362-9897; e-mail: wlee@spin.yonsei.ac.kr); Dai Woon Lee, Ph.D. (Tel: +82-2-2123-2635, Fax: +82-2-364-7050; e-mail: leedw@yonsei.ac.kr)

Ser[1]-Gly[2]-Arg[3]-Gly[4]-Lys[5]-Gly[6]-Gly[7]-Lys[8]-Gly[9]-Leu[10]-Gly[11]-Lys[12]-Gly[13]-Gly[14]-

Ala[15]-Lys[16]-Arg[17]-His[18]-Arg[19]-Lys[20]-Val[21]-Leu[22]-Arg[23]-Asp[24]-Asn[25]-Ile[26]-Gln[27]

Figure 1. The primary sequence of N-terminal region of histone H4. All acetylation sites of H4 are indicated as circles.

ranges of 1.8-7.0 by addition of 1 N NaOH. All NMR experiments were performed on a Bruker AMX500 or DRX500 spectrometer in quadrature detection mode equipped with a triple resonance probe having an actively shielded pulsed-field gradient (PFG) coil. Most of experiments were performed at temperatures of 5 and 25 °C. Two-dimensional

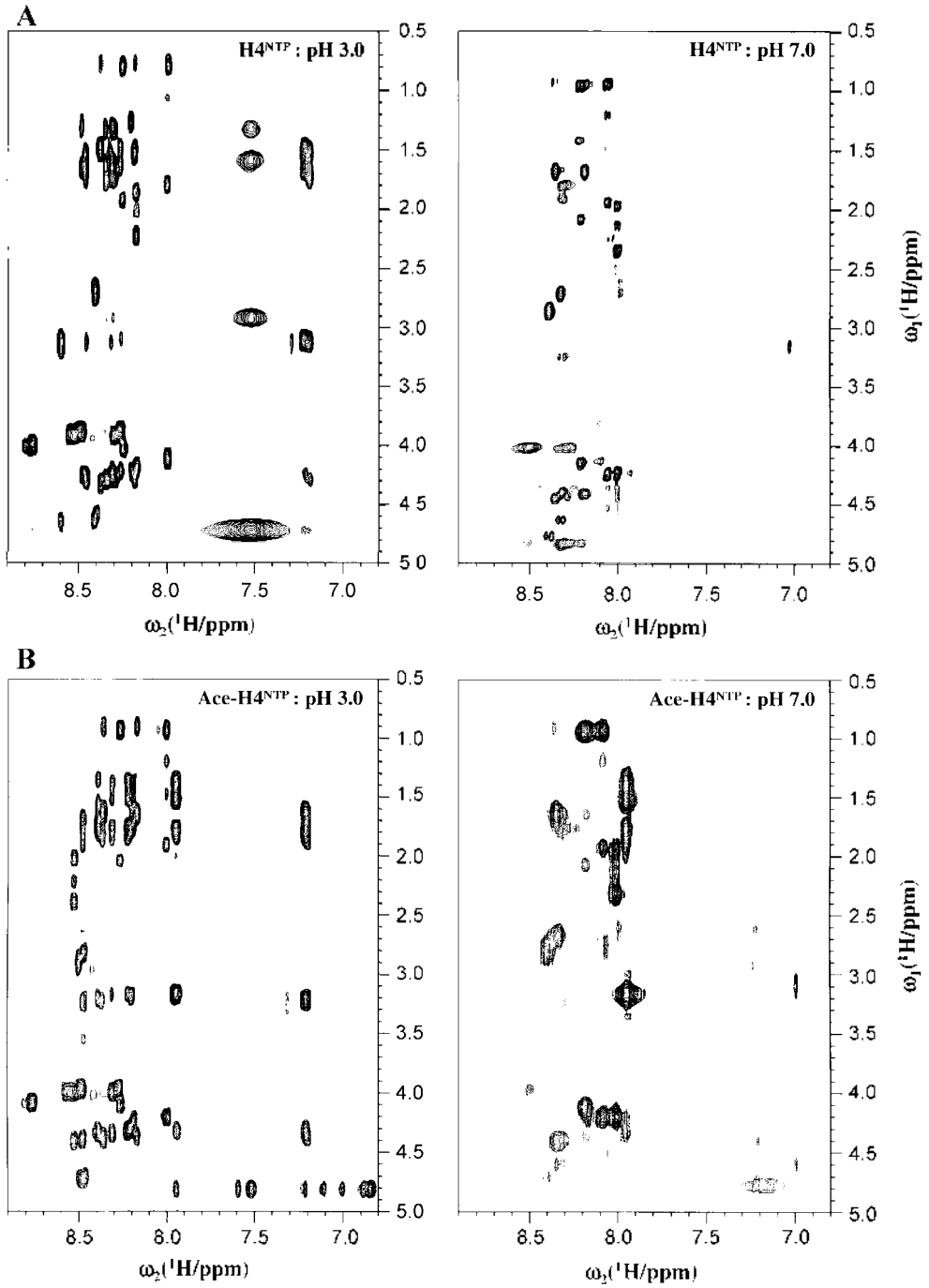

Figure 2. 2D-TOCSY spectra of both $H4^{NTP}$ (A) and Ace-$H4^{NTP}$ (B) at pH values of 3.0 and 7.0, at 25 °C.

(2D) NMR spectra were recorded in phase-sensitive mode using time-proportional phase increment (TPPI)[14] for quadrature detection in the t_1 domain. Nuclear Overhauser enhancement spectroscopy (NOESY)[15] with mixing times of 400 and 600 ms was performed. Double quantum filtered correlation spectroscopy (DQF-COSY)[16] and total correlation spectroscopy (TOCSY)[17] using MLEV-17 spin lock pulse sequence with a mixing time of 48 ms were also performed. For DQF-COSY experiments, solvent suppression was achieved using selective low power irradiation of the water resonance during 2s of relaxation delay. Solvent suppression for TOCSY and NOESY experiments was achieved using WATERGATE pulse sequence[18] combined with PFG pulses. All NMR spectra were acquired with 2048 complex data points in t_2 and 256 increments in the t_1 dimension. All NMR data were processed using nmrPipe/nmrDraw (Biosym/Molecular Simulations, Inc.) or XWIN-NMR (Bruker Instruments) software on a Silicon Graphics Indigo^2 workstation and analyzed using the Sparky 3.60 program.

Structure Calculations. Solution structures were calculated using the hybrid distance geometry and dynamical simulated-annealing methods[19-22] with the program XPLOR 3.1 (Biosym/Molecular Simulations, Inc.). All calculations were carried out on a Silicon Graphics Indigo^2 workstation using the topology and parameter files of topallhdg.pro and parallhdg.pro. The methodology used was similar with the original protocol of Lee *et al.*.[23] The target function of NOEs is used in the same manner described in Driscoll *et al.*[24] The target function for molecular dynamics and energy minimization consisted of covalent structure, van der Waals repulsion, NOE and torsion angle constraints. A total of 56 distance restraints and 7 dihedral restraints for H4^{NTP} were used for structural calculations, and 52 distance restraints and 5 dihedral restraints for Ace-H4^{NTP} were used. Distance restraints were classified as strong (1.8-2.5 Å), medium (1.8-3.0 Å) and weak (1.8-5.0 Å) based on observed NOE intensities. Appropriate pseudoatom corrections were applied to non-stereo specifically assigned methylene and methyl protons.[25] In addition, 1.0 Å was added to the upper limit of distances involving methyl protons. Final structures were displayed and analyzed using Insight II (Biosym/Molecular Simulations, Inc.) and MOLMOL programs.[26]

Results and Discussion

Conformational Changes for Different pH Values. A series of 1D and 2D-TOCSY spectra were obtained to investigate conformational change for both H4^{NTP} and Ace-H4^{NTP} peptides at pH values of 3.0-7.0. Figure 2 shows TOCSY spectra at pH values of 3.0 and 7.0, demonstrating spectral changes. In different pH environments, chemical shift changes were observed due to both protonation (the side chain amino groups of Lys and Arg residues and the ring protons 2H and 4H of His residue) and deprotonation (Gln27 amide proton) process.[27] It is also interesting to see that the side-chain amino groups of Lys residues in Ace-H4^{NTP} did not shift much even at high pH mainly due to acetylation. Especially, most of the amide resonances of Ace-H4^{NTP} became broad due to both the fast base-catalyzed proton exchanges at neutral pH and conformational change by acetylation process.

NMR Resonance Assignments. Spin system and sequential assignments of H4^{NTP} were achieved using the standard

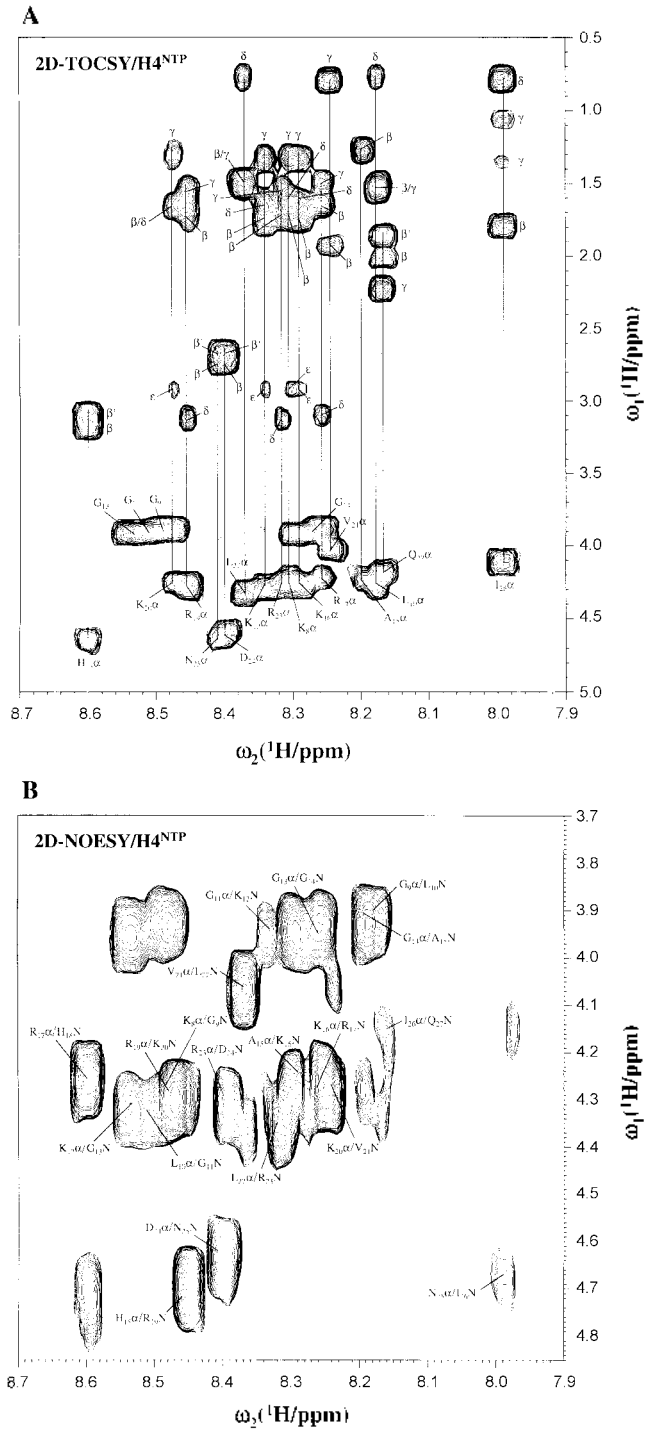

Figure 3. (A) 2D-TOCSY spectrum of H4^{NTP} with mixing time of 48ms at pH 3.0, 25 °C. (B) 2D-NOESY spectra of H4^{NTP} at pH 3.0 and 25 °C in finger print region was displayed. The NOE mixing time of 600ms was used for this experiment.

Table 1. Proton NMR chemical shift assignments for $H4^{NTP}$. Chemical shifts are expressed in ppm. The sample was maintained at 25 °C, pH 3.0

Residue	NH	$C^{\alpha}H$	$C^{\beta}H$	Other
Lys8	8.31	4.27	1.81, 1.71	$C^{\gamma}H$ (1.37) $C^{\delta}H$ (1.62) $C^{\varepsilon}H$ (2.94) εNH (7.52)
Gly9	8.49	3.90		
Leu10	8.18	4.27	1.57, 1.57	$C^{\gamma}H$ (1.57) $C^{\delta}H$ (0.83)
Gly11	8.51	3.91		
Lys12	8.34	4.28	1.83, 1.72	$C^{\gamma}H$ (1.39) $C^{\delta}H$ (1.67) $C^{\varepsilon}H$ (2.94) εNH (7.52)
Gly13	8.53	3.93		
Gly14	8.27	3.90		
Ala15	8.20	4.24	1.32	
Lys16	8.29	4.27	1.81, 1.71	$C^{\gamma}H$ (1.37) $C^{\delta}H$ (1.62) $C^{\varepsilon}H$ (2.94) εNH (7.52)
Arg17	8.26	4.23	1.70	$C^{\gamma}H$ (1.54) $C^{\delta}H$ (3.12) NH (7.21, 6.64)
His18	8.60	4.66	3.20, 3.12	2H (8.61) 4H (7.24)
Arg19	8.46	4.28	1.73	$C^{\gamma}H$ (1.60) $C^{\delta}H$ (3.14) NH (7.19, 6.64)
Lys20	8.48	4.27	1.74, 1.68	$C^{\gamma}H$ (1.36) $C^{\delta}H$ (1.68) $C^{\varepsilon}H$ (2.95) εNH (7.52)
Val21	8.24	4.04	1.97	$C^{\gamma}H$ (0.88, 0.83)
Leu22	8.37	4.33	1.55, 1.55	$C^{\gamma}H$ (1.55) $C^{\delta}H$ (0.84)
Arg23	8.32	4.27	1.72	$C^{\gamma}H$ (1.58) $C^{\delta}H$ (3.14) NH (7.19, 6.64)
Asp24	8.40	4.62	2.74, 2.68	
Asn25	8.41	4.65	2.75, 2.67	γNH (7.50, 6.76)
Ile26	7.99	4.12	1.83	$C^{\gamma}H$ (1.39, 1.10) $C^{\delta}H$ (0.84)
Gln27	8.17	4.19	2.06, 1.90	$C^{\gamma}H$ (2.26) $^{\varepsilon}NH$ (7.57, 6.81)

assignment procedure.[28] Spin system assignments were easily made with TOCSY spectra (Figure 3A). Due to severe spectral overlaps at pH 7.0, the complete assignments were performed at low pH. Single Ala, His, Val, Asp, Asn, Ile, Gln, and two Leu residues were easily identified by their characteristic connectivities on TOCSY spectrum. However, because of three repetitions of Gly-Lys-Gly sequence and the unusual string of many basic Lys and Arg residues, the resonances of N-terminal regions particularly are seriously overlapped. Sequential assignment for the backbone protons was completed by following $d_{\alpha N}$(i,i+1) connectivities starting from NH-$C^{\alpha}H$ cross peaks of known amino acids on NOESY spectra. The side chain proton resonances were identified from TOCSY connectivities (Figure 3A) and proton chemical shifts for $H4^{NTP}$ at 25 °C are summarized in Table 1. A continuous stretch of $d_{\alpha N}$(i,i+1) sequential NOEs

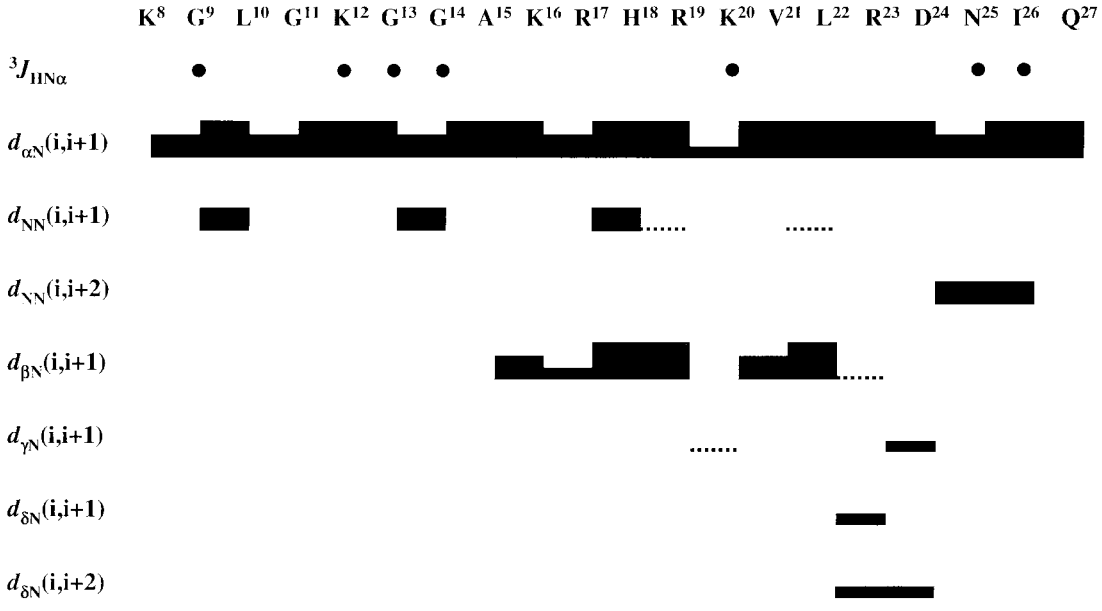

Figure 4. Summary of NMR data for $H4^{NTP}$ showing the sequential and short-range NOE connectivities at pH 3.0. Observed NOE intensities are classified by the thickness of the lines. Ambiguous NOEs were marked as (---). Backbone vicinal coupling constants (●; $^3J_{HN\alpha}$ < 6 Hz) are indicated.

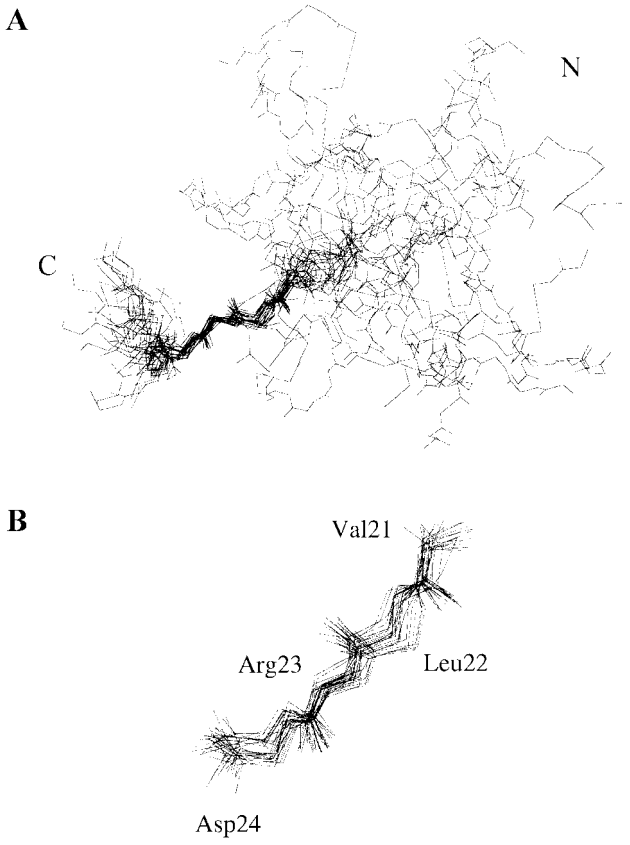

Figure 5. Final simulated annealing structures of backbone atoms for $H4^{NTP}$, showing that (A) converged regions of Val21-Asp24, and (B) local superimposed structure for well-defined region spanning residues of Val21-Asp24.

was shown in Figure 3B. We could observe four NH/NH NOEs for residues of Gly9-Leu10, Gly13-Gly14, Arg17-His18, and Asp24-Ile26. Figure 4 summarizes the sequential and short-range NOE connectivities for the $H4^{NTP}$ at pH 3.0. For acetylated $H4^{NTP}$, strong acetyl CH_3 resonances were detected at 2.0 ppm by acetylation of the ε-amino group of the Lys residues and the $N^{\varepsilon}H$ resonances of Lys were shifted to downfield from acetylation (from 7.56 to 7.95 ppm).

Solution Structure of $H4^{NTP}$. The solution structure was calculated from the NMR experimental restraints. Among 50 dynamical simulated-annealing structures, 27 structures showed no violations greater than 0.5 Å for distance and 5° for torsion angle. The average structure was calculated from 27 final structure coordinates and followed restrained energy minimization procedure, generating a restrained energy minimized (REM) averaged structure of $H4^{NTP}$ ($<\overline{SA}>_{kr}$) (Figure 5A). Solution structures indicated that the region of Lys20-Asn25, especially Val21-Asp24 were relatively well-defined, having that root-mean square deviation (RMSD) values of backbone atoms for these regions are 1.34 Å and 0.89 Å. Local superimposed structure for the region of Val21-Asp24 was shown in Figure 5B. Energies and structural statistics for 27 final simulated annealing structures are listed in Table 2. It has been reported that the highly basic N-terminal region comprising residues of 1-25 has ability to bind to a region of extreme acidity on the exposed face of the H2A-H2B dimer in nucleosome core particle by Luger *et al.*[29] They pointed that the region comprising from Lys16 to Asn25 contains multiple hydrogen bonds and salt bridges between basic side chains of H4 (Lys16, Arg19, Lys20, Arg23) and acidic side chains of H2A (Glu56, Glu61,

Table 2. Structural Statistics[a] for the 27 Final Simulated Annealing Structures of $H4^{NTP}$

Parameter	$<SA>_k$	$<\overline{SA}>_{kr}$
rms deviations from experimental distance restraints (Å)		
all (56)	0.052 (0.043-0.062)[a]	0.097
sequential ($\|i-j\|=1$) (34)	0.064 (0.054-0.077)	0.124
short-range ($1<\|i-j\|\leq 5$) (2)	0.032 (0-0.146)	0
long-range ($\|i-j\|>5$) (0)	–	–
intraresidue (20)	0.014 (0 0.044)	0.008
hydrogen bond (0)	–	–
rms deviations from experimental dihedral restraints		
dihedral restraints (deg) (7)	0.065 (0-0.427)	0.093
energies		
$E_{overall}$ (kcal mol^{-1})	34.440 (29.630-39.300)	32.655
E_{NOE} (kcal mol^{-1})	7.658 (5.090-10.720)	5.572
E_{repel} (kcal mol^{-1})	0.98 (0.069-2.466)	0.855
E_{cdih} (kcal mol^{-1})	0.009 (0-0.078)	0
E_{L-J} (kcal mol^{-1})[b]	-47.709 (-3.024—88.580)	-9.75
deviations from idealized covalent geometry		
bonds (Å)	2.114×10^{-3} (1.717×10^{-3}-2.446×10^{-3})	1.813×10^{-3}
angles (deg)	0.483 (0.460-0.507)	0.494
impropers (deg)	0.331 (0.313-0.355)	0.324

[a]The values are averages of 27 structures of $H4^{NTP}$. The $<SA>_k$ structures were generated from 50 initial structures by simulated annealing protocol with subsequent refinement. [b]The numbers in parentheses represent minimum and maximum values. [c]E_{L-J} represents the Lennard-Jones potential energy.

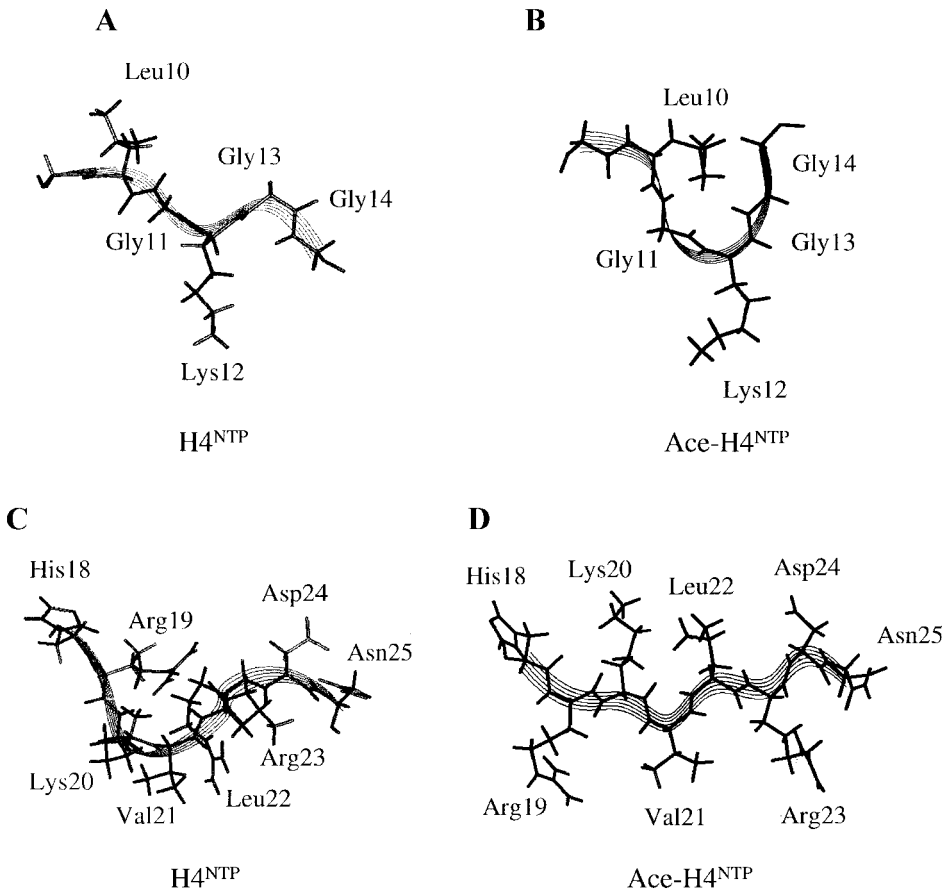

Figure 6. REM structures for $H4^{NTP}$ and Ace-$H4^{NTP}$: (A) the regions of Leu10-Gly14 for $H4^{NTP}$, and (B) equivalent regions of Ace-$H4^{NTP}$ whereas (C) the region of His18-Asn25 for $H4^{NTP}$ and (D) that of Ace-$H4^{NTP}$, respectively.

Glu64, Asp90, Glu91, Glu92) and H2B (Glu110). It is thought that the affinity between charged residues by the H4 tail would be favored at low pH and it is reduced by successive acetylation of the H4 Lys5, Lys8, Lys12 and Lys16. Our data in this report reveals that $H4^{NTP}$ has a defined structure for residues of Val21-Asp24 at lower pH conditions, though it did not possess any defined structures at physiological pH (Figure 6C). It has been proposed that acetylation of the Lys residues abolishes the interaction with DNA, resulting in conformational change of chromatin to more extended form.[30,31] Especially, we observed that Lys12 residue may play an important role for its structural change upon acetylation.[5,30,32] In our study, although there are no significant conformational changes, acetylation at Lys residues induces defined structures in the regions of Leu10-Gly13 and Arg19-Leu22 (Figure 6). Based on 2D-NOESY spectra, the NOE pattern of Ace-$H4^{NTP}$ is similar to that of $H4^{NTP}$. However two additional NH/NH NOEs between Gly11-Lys12, and Lys12-Gly13 which were not detected in $H4^{NTP}$ were clearly observed in acetylated peptide. Therefore, we conclude that an extended conformation of $H4^{NTP}$ is important for active acetylation procedure. After acetylation, the region containing lysine residues (especially Lys12) became a defined structure, presumably due to neutralization and reduction of repulsion force between the positive charges of the $H4^{NTP}$.

Acknowledgment. The authors wish to acknowledge the financial support of the Korean Research Foundation made in the program year of 1998 (W. Lee and J. Yoon. 1998-001-D00551).

References

1. Wolffe, A. P. *Chromatin: Structure and Function*; Academic Press: London, 1998.
2. Schild, C.; Claret, F.-X.; Wahli, W.; and Wolffe, A. P. *EMBO J.* **1993**, *12*, 423-433.
3. Brownell, J. B.; Allis, C. D. *Curr. Opin. Genet. Dev.* **1996**, *6*, 176-184.
4. Braunstein, M.; Rose, A. B.; Holmes, S. G.; Allis, C. D.; Broach, J. R. *Genes Dev.* **1993**, *7*, 592-604.
5. Braunstein, M.; Sobel, R. E.; Allis, C. D.; Turner, B. M.; Broach, J. *Mol. Cell. Biol.* **1996**, *16*, 4349-4356.
6. Wolffe, A. P. *Science* **1996**, *272*, 371-372.
7. Kleff, S.; Andrulis, E. D.; Anderson, C. W.; Sternglanz, R. *J. Biol. Chem.* **1995**, *270*, 24674-24677.
8. Brownell, J. E.; Zhou, J.; Ranalli, T.; Kobayashi, R.; Edmondson, D. G.; Roth, S. Y.; Allis, C. D. *Cell* **1996**, *84*, 843-851.
9. Taunton, J.; Hassig, C.A.; Schreiber, S. L. *Science* **1996**, *272*, 408-411.
10. Allfrey, V. G.; Faulkner, R. M.; Mirsky, A. E. *Proc. Natl. Acad. Sci. USA* **1964**, *51*, 786-794.

11. Clarke, D. J.; ONeill, L. P.; Turner, B. M. *Biochem J.* **1993**, *294*, 557-561.
12. O'Neill, L. P.; Turner, B. M. *EMBO J.* **1995**, *14*, 3946-3957.
13. Sobel, R. E.; Cook, R. G.; Perry, C. A.; Annunziato, A. T.; Allis, C. D. *Proc. Natl. Acad. Sci. USA* **1995**, *92*, 1237-1241.
14. Marion, D.; Wuthrich, K. *Biochem. Biophys. Res. Commun.* **1983**, *113*, 967-974.
15. Jeener, J.; Meier, B. H.; Bachman, P.; Ernst, R. R. *J. Chem. Phys.* **1979**, *71*, 4546-4553.
16. Rance, M.; Sorensen, O. W.; Bodenhausen, G.; Wagner, G.; Ernst, R. R., Wuthrich, K. *Biochem. Biophys. Res. Commun.* **1983**, *117*, 479-485.
17. Davis, D. G.; Bax, A. *J. Am. Chem. Soc.* **1985**, *107*, 2820-2821.
18. Piotto, M.; Saudek, V.; Sklenar, V. *J. Biomol. NMR* **1992**, *2*, 661-665.
19. Driscoll, P. C.; Gronenborn, A. M.; Beress, L.; Clore, G. M. *Biochemistry* **1989**, *28*, 2188-2198.
20. Nilges, M.; Clore, G. M.; Gronenborn, A. M. *FEBS Lett.* **1988**, *229*, 317-324.
21. Nilges, M.; Clore, G. M.; Gronenborn, A. M. *FEBS Lett.* **1988**, *239*, 129-136.
22. Nilges, M.; Gronenborn, A. M.; Brunger, A. T.; Clore, G. M. *Protein Eng.* **1988**, *2*, 27-38.
23. Lee, W.; Moore, C. H.; Watt, D. D.; Krishna, N. R. *Eur. J. Biochem.* **1994**, *218*, 89-95.
24. Driscoll, P. C.; Gronenborn, A. M.; Clore, G. M. *FEBS Lett.* **1989**, *243*, 223-233.
25. Wuthrich, K.; Billeten, M.; Braun, W. *J. Mol. Biol.* **1983**, *169*, 949-961.
26. Koradi, R.; Billeter, M.; Wuthrich, K. *J. Mol. Graphics* **1996**, *14*, 51-55.
27. Vu, H. M.; Minch, M. J. *J. Peptide Res.* **1998**, *51*, 162-170.
28. Wuthrich, K. *NMR of Proteins and Nucleic Acids*; Wiley: New York, 1986.
29. Luger, K.; Mader, A. W.; Richmond, R. K.; Sargent, D. F.; Richmond, T. J. *Nature* **1997**, *389*, 251-260.
30. Dutnall, R. N.; Tafrov, S. T.; Sternglanz, R.; Ramakrishnan, V. *Cell* **1998**, *94*, 427-438.
31. Cary, P. D.; Crane-Robinson, C.; Bradbury, E. M.; Dixon, G. H. *Eur. J. Biochem.* **1982**, *127*, 137-143.
32. Turner, B. M.; Birley, A. J.; Lavender, J. *Cell* **1992**, *69*, 375-384.